MOLECULAR IMAGING AND BIOLOGY

RESEARCH ARTICLE

Non-invasive Optical Imaging of Muscle Pathology in *mdx* Mice Using Cathepsin Caged Near-Infrared Imaging

Andreas R. Baudy,[1,2] Arpana Sali,[1] Sarah Jordan,[1] Akanchha Kesari,[1] Helen K. Johnston,[1,2] Eric P. Hoffman,[1,2] Kanneboyina Nagaraju[1,2]

[1]*Research Center for Genetic Medicine, Children's National Medical Center, Washington DC, USA*
[2]*Department of Integrative Systems Biology, George Washington University School of Medicine and Health Sciences, Washington DC, USA*

Abstract

Purpose: To develop a reliable live-animal imaging method for monitoring muscle pathology in mouse models of myopathy.
Procedures: A caged near-infrared Cathepsin B (CTSB) substrate, ProSense 680, is evaluated in the dystrophin deficient *mdx* mice, a genetic homologue of Duchenne muscular dystrophy via optical imaging.
Results: We show high levels of infrared signal in dystrophic muscle relative to healthy muscle at 24 h post-injection. Imaging for CTSB presence revealed localization to inflammatory infiltrates and regenerating muscle fibers. A time series myotoxin-induced muscle injury experiment showed that CTSB activity and its mRNA levels peaked at the interface between inflammation and myoblast fusion stage of recovery. Prednisone treatment in *mdx* mice resulted in decreased CTSB activity and increased grip strength in forelimbs and hindlimbs.
Conclusions: Optical imaging of CTSB activity is an ideal method to sensitively monitor inflammation, regeneration, and response to therapy in myopathic skeletal muscle.

Key words: Live optical imaging, Duchenne muscular dystrophy, *mdx*, Cathepsin B, Muscle inflammation

Abbreviations: DMD, Duchenne muscular dystrophy; CTSB, Cathepsin B

Introduction

Pre-clinical trials in animal models of muscle disease are a critical step in drug development. The most widely

used genetic and biochemical model for Duchenne muscular dystrophy (DMD) is the *mdx* mouse [1–3]. However, it has a relatively mild disease phenotype compared to the progression of disease seen in human patients, and so establishing reliable and sensitive outcome measures for pre-clinical drug trials using this model has been challenging.

The availability of live-animal imaging accelerates the discovery of effective therapeutics in pre-clinical and clinical trials because it can deliver a variety of useful pathophysiological information in a longitudinal manner. Magnetic resonance imaging has been the primary imaging modality successful at detecting muscle pathology, but it has several limitations including cost, sensitivity for changes in muscle tissue, speed of operation, and compliance of awake children [4–6]. An alternative approach is the use of optical probes, such as caged near-infrared enzyme substrates, where imaging can be done using optical systems [7].

In DMD, dystrophin deficiency results in plasma membrane abnormalities, with increased susceptibility to contraction-induced myofiber damage, and bouts of myofiber degeneration and regeneration [1, 8]. Inflammatory cells are a feature of dystrophic muscle, although the muscle is heterogeneous, with different regions showing degeneration, regeneration, and inflammation [9]. In fact, tissue heterogeneity is a major limitation in using muscle biopsies to monitor efficacy of pre-clinical and clinical trials. Since regeneration and inflammation are critical disease components in DMD, the identification of an optical probe reflecting both of these processes would have the potential to be a sensitive and reliable surrogate biomarker relaying overall disease status within the muscle tissue.

The cathepsins are a family of 11 proteases that are expressed in most cell types and generally become cleaved and activated in low pH environments such as in the lysosomes [10]. Cathepsin B (CTSB) is a cysteine protease that has previously been shown to be upregulated in DMD patient muscle, primarily localizing to macrophage infiltrating areas [11, 12]. CTSB is initially translated as an inactive 44 kDa precursor protein, but can be activated into a mature 33 kDa single-chain enzyme [13]. CTSB is highly upregulated in activated fusing myoblasts and hypothesized to be a major contributor to the process of extracellular matrix remodeling, which is an essential step in muscle regeneration [14].

Here, we investigate the use of a CTSB substrate as a live-animal imaging method to assess muscle pathology. We show that optical imaging of CTSB enzyme activity using a caged near-infrared substrate (ProSense 680) is capable of effectively detecting muscle inflammation, regeneration, and response to therapy in the *mdx* model via optical imaging.

Materials and Methods

Patient Expression Biopsies

DMD patient populations in this study were drawn from a referral population. Flash-frozen muscle biopsies from patients with a tentative diagnosis of muscular dystrophy were sent to the Dr. Hoffman's laboratory at Children's National Medical Center, Washington DC. All biopsies were subjected to a standardized set of biochemical and histological assays, including immunostaining for dystrophin, alpha-sarcoglycan and merosin, and immunoblotting for dystrophin and dysferlin. All samples were analyzed under CNMC IRB protocol #2405 which has been reviewed and approved by the Office for the Protection of Human Subjects at Children's National Medical Center. Dystrophin immunostaining and mRNA expression profiling were performed as described previously [15, 16] and analysis criteria was set to only include patients over 2 years of age.

Mice

C57bl/10ScSn-*Dmd*^{mdx}/J (*mdx*) and control C57bl/10 (bl10) mice were purchased from Jackson Laboratory (Bar Harbor, ME) and all animal experiments were conducted in accordance with our IACUC guidelines under approved protocols.

Optical Imaging

Five-week-old *mdx* and bl10 mice that underwent optical imaging were first put under gas anesthesia using 4% isofluorane and 0.5 L/min 100% oxygen, placed inside an Optix MX2 Imager (ART) scanning chamber, and then anesthesia was maintained with 2% isofluorane and 0.5 L/min oxygen through a nose cone to the mice. The floor of the scanning chamber in which the mouse lies was heated in order to maintain normal physiological body temperatures. Hair covering areas to be scanned was removed with Nair. The plane of scanning was kept consistent between mice at the level immediately above the forelimbs. Mice underwent intra-peritoneal (I.P.) injection with 0.75 nmol or 1.5 nmol of ProSense 680 (VisEn Medical), both prepared in a total volume of 150 µl phosphate-buffered saline (PBS). Areas of scanning were defined with a polygonal selection tool, then a 670 nm excitation laser was used for probe excitation at a 1.5-mm camera resolution in the whole body scanning experiments (*n*=2/group), and at a 0.5-mm camera resolution in skeletal limbs (*n*=3/group); emissions were collected from a 700-nm long-pass filter. After scanning, the mice were allowed to recover under 0.5 L/min oxygen. Optical-imaging intensities from all experiments were normalized to account for differences in scanning laser power, integration times, and scanning area selected between mice using Optiview 2.0 software.

Histology and Immunofluoresence

Quadriceps from *mdx* mice were isolated and frozen in liquid nitrogen-cooled isopentane, 8-µm frozen sections were prepared, and unfixed cryosections from ProSense-injected mice were scanned with a 635-nm excitation laser, and then subsequently stained with Hematoxylin and Eosin (H&E). Notexin-injured gastrocnemius muscles (see below) from bl10 mice were isolated and sectioned in the same manner, blocked in 10% horse serum (HS) diluted in PBS for 30 min, then incubated with Hoechst dye (Sigma Aldrich, 1:10,000), anti-laminin (Sigma Aldrich, 1:200), anti-embryonic myosin heavy-chain (University of Iowa Hybridoma Bank, 1:200), and anti-F4/80 (Serotec, 1:200) antibodies for 2 h at room temperature. The sections were washed three times with PBS, and then Cy2 (Jackson Immunoresearch, 1:500) and Alexafluor: 546, 633 (Invitrogen, 1:500) secondary antibodies were prepared in 10% HS diluted in PBS and applied for 1 h, then the sections were washed three times with PBS, and mounted with permount (Fisher Scientific). The sections were visualized using a LSM 510 confocal microscope (Zeiss).

Myotoxin Injury

mRNA profiles were analyzed for CTSB expression from a previously published study in which cardiotoxin was administered via intramuscular (I.M.) injection into the gastrocnemious muscle of bl10 mice [16]. For the in vitro experiments notexin (Latoxin) was prepared at a concentration of 4 µg/ml in 70 µl of 0.9% NaCl and administered via I.M. injection into the right medial region of the gastrocnemius muscle of bl10 mice, and 0.9% NaCl was administered to the contralateral leg in the same region. Mice were divided into post-notexin injection days 1, 3, 5, and 14 subsets (*n*=3/group) and all received a single injection I.P. of 1.5 nmol ProSense 680 24 h prior to imaging.

Prednisone Treatment

Eight-week-old *mdx* mice were split into untreated and prednisone treated groups (*n*=3/group); the treated group received prednisone in time-release pellets (Innovative Research, 1 mg/kg), which were implanted subcutaneously to establish continuous drug delivery. After 3 weeks of administration, all mice were scanned for baseline levels of optical intensity, injected with 1.5 nmol of ProSense I.P, then 24 h later, both forelimbs and hindlimbs were scanned at 0.5-mm resolution and quantified using Optiview software. Grip strength was assessed using a grip-strength meter (Columbus instruments, Columbus, Ohio). Five successful hindlimb- and forelimb-strength measurements were recorded over a period of 2 min. The grip-strength measurements were collected in the morning hours over a 5-day period; the maximum values of each day over the 5-day period were used for subsequent analysis. Both grip strength and optical-imaging intensities were normalized directly to body weight.

Statistical Analysis

Sample size calculations used a student's *t* distribution to determine the number of mice per group needed to detect a significant difference between untreated and prednisone chronic treatment. The same method was used to determine sample sizes necessary to detect a significant difference in normalized forelimb/hindlimb measurements. All calculations assumed an alpha level of 0.05 and a power level of 80%.

Results

Cathepsin B Shows High Expression in Duchenne Muscular Dystrophy Patient Muscle

Thirteen muscle biopsies from DMD patients and six biopsies from non-dystrophic control patients were evaluated by microarray transcriptional analysis, then queried for four CTSB probe sets, which represented the entire range of CTSB transcripts (see Supplementary Fig. 1 online). Twelve of the 13 DMD biopsies had upregulated CTSB levels in at least one of the four probe sets, and the majority of biopsies had upregulated CTSB levels in at least three of the four probe sets. DMD patient biopsy three was the primary outlier in the analysis, since CTSB was entirely downregulated. Five of the
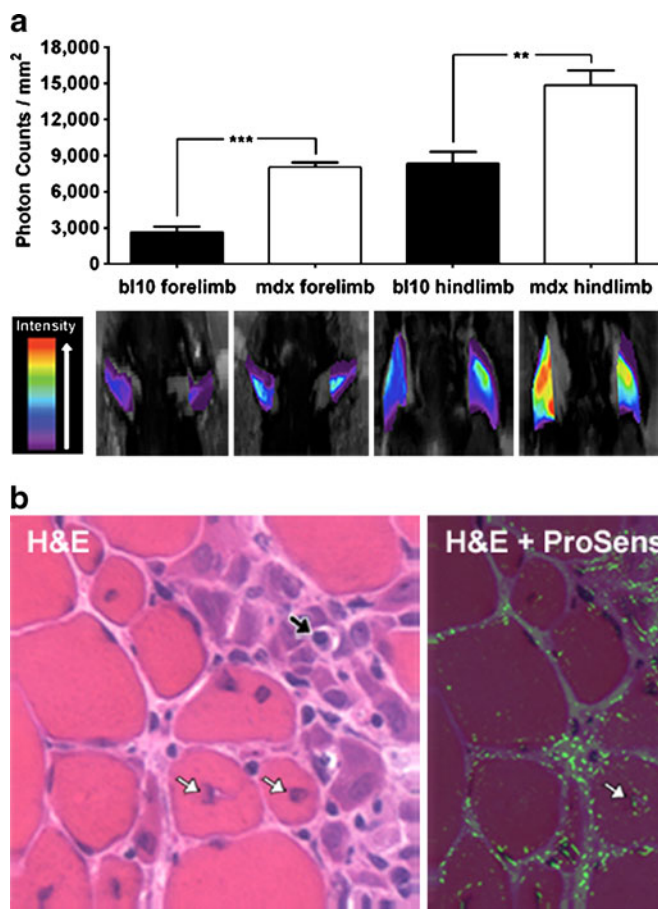

Fig. 1. CTSB activity and localization in limb muscles 24 h post-Prosense 680 injection. Optical imaging performed at 0.5 mm resolution of the limb muscles in *mdx* and bl10 mice (**a**). CTSB was activated 3.15-fold more in *mdx* forelimb compared to bl10 and 1.85-fold more in hindlimb (Student's *t* test, showing standard error of the mean, *******p* value=0.0017, ********p* value=0.0001). Frozen cross-sections of quadriceps muscle taken from *mdx* mice were visualized in the near-infrared (*green*), then subsequently stained with H&E (**b**). CTSB signal was highly specific to areas containing regenerating fibers, illustrated by *white arrows*, and inflammatory foci illustrated by *black arrow*.

six non-dystrophic control group biopsies were downregulated for CTSB transcript, with only control patient biopsy six showing upregulation.

I.P. Injection of Caged Near-Infrared CTSB Substrate Detects Cathepsin Activity in Dystrophic Muscle

ProSense 680 is a small peptide substrate for activated CTSB [17]. When cleaved by the CTSB enzyme, two caged fluorophores are released, with peak excitation at 680 nm, and emission in the near-infrared range (700 nm). Intraperitoneal injection of 1.5 nmol or 0.75 nmol ProSense 680 was done in 5-week-old wild-type bl10 and dystrophin-deficient *mdx* mice. Serial optical whole body scanning at a 1.5-mm camera step resolution demonstrated near-infrared signal in the liver and bladder at 6 h that was similar between dystrophic and control mice (see Supplementary Fig. 2a online). Signal corresponding to limb muscle was observed more specifically in the dystrophic mice with a plateau at 24–48 h. The average total limb photon intensity was quantified for both bl10 and *mdx* mice that were injected with either 1.5 or 0.75 nmol over time (see Supplementary Fig. 2b online).

Based on this time course data, all further experiments were performed using the 1.5 nmol dose of ProSense, with scanning performed 24 h after injection. A group of age matched (5-week-old) *mdx* and bl10 wild-type mice ($n=3$ per group) were injected with 1.5 nmol ProSense and a single scan was performed of solely the forelimb and hindlimb. We found significant increases in CTSB photon count intensity in the *mdx* forelimb (3.1-fold increase) relative to bl10, as well as in the hindlimb (1.9-fold increase) (Fig. 1a). After imaging, mice were euthanized then cryosections of their quadriceps were exposed for near-infrared signal, subsequently stained with H&E, and both images superimposed. CTSB activity was localized to both centrally nucleated regenerating fibers (*white arrows*), as well as inflammatory cells (*black arrow*) (Fig. 1b).

Myotoxin-Induced Regeneration Stimulates CTSB Transcription, with Peak at Myoblast/Myotube Transition

Zhao et al. [18] previously had investigated myofiber damage in the gastrocnemius of bl10 mice using micro-array transcriptional analysis of myotoxin-damaged tissues. CTSB-transcript activity significantly increased between days 2–6, with a peak at day 3 (Fig. 2a). We followed-
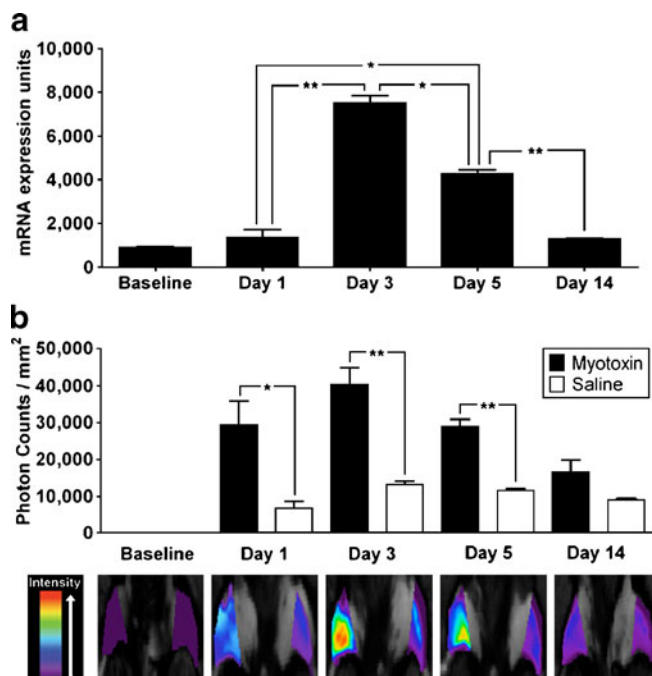

Fig. 2. CTSB is strongly expressed on mRNA and activated at protein levels in myotoxin-damaged muscle. bl10 mice were injured with I.M. injection of myotoxin into the gastrocnemius, and microarray expression analysis was subsequently performed. **a)** Analysis of two representative CTSB probes (92256_at and 95608_at, shown as an average) revealed slight mRNA upregulation at day 1, with peak levels at day 3 and a decline back to near baseline by day 14. (Student's *t* test, showing standard error of the mean, * *p* value of day 3 and day 5=0.0127, for day 1 and day 5=0.0175; **p* value for day 5 and day 14= 0.0035, for day 1 and day 3=0.0060). **b)** CTSB caged optical imaging in the hindlimbs of myotoxin injured bl10 mice revealed a drastic increase of CTSB activity at day 1, with a peak at day 3, and resolution by day 14 (Student's *t* test, showing standard error of the mean, *p* value day 1=0.0303, **p* value day 3=0.0046, day 5=0.0012).

up with these results with another group of bl10 mice by administering I.M. injections of saline into the left leg gastrocnemious and myotoxin in the right leg gastrocnemious of all mice, which were then imaged on days 1, 3, 5, and 14 post-injection. A rapid increase of activated CTSB levels in the injured leg was observed at post-myotoxin injection day 1, followed by a peak at day 3, and resolution of activity by day 14 (Fig. 2b). Injured gastrocnemious muscles taken from day 5 exhibited inactive precursor CTSB co-localization primarily to macrophages (Fig. 3), whereas activated CTSB was observed both in macrophages and in regenerating fibers (Fig. 4).

Therapeutic Response can be Successfully Evaluated in the mdx Mouse with CTSB Imaging

We tested the sensitivity of our method to detect therapeutic benefits induced by prednisone, the current standard of treatment for DMD patients, in the *mdx* model. A prednisone pellet was placed subcutaneously for continuous dosing for a total of 3 weeks, and then CTSB optical imaging and grip-strength analysis were performed at endpoint (Fig. 5). We observed a $49.7 \pm 10.9\%$ reduction of CTSB signal in the forelimbs and $25.9 \pm 9.7\%$ reduction in hindlimbs (Fig. 5a), as well as a $14.7 \pm 2.2\%$ increase in forelimb strength and a $21.9 \pm 2.5\%$ increase in hindlimb strength (Fig. 5b).

Statistical Analysis Demonstrates Excellent Sensitivity in Detecting Strain and Drug Treatment Differences

Statistical calculations based on the mean and standard deviations predicted that the assay is highly sensitive in detecting differences between *mdx* and bl10 strains, with only one mouse required per group to detect differences in the forelimbs, and three mice required per group to detect differences in the hindlimbs (Table 1). The sensitivity for monitoring prednisone-induced drug benefits was also excellent for detecting differences in the forelimbs, requiring only two mice per group, but more modest in the hindlimbs, requiring six mice per group (Table 2).

Discussion

Our goal was to define an optical-imaging method that could comprehensively capture muscle pathology in the *mdx* model, so as to improve the effectiveness of monitoring therapeutic intervention in pre-clinical studies. Since we
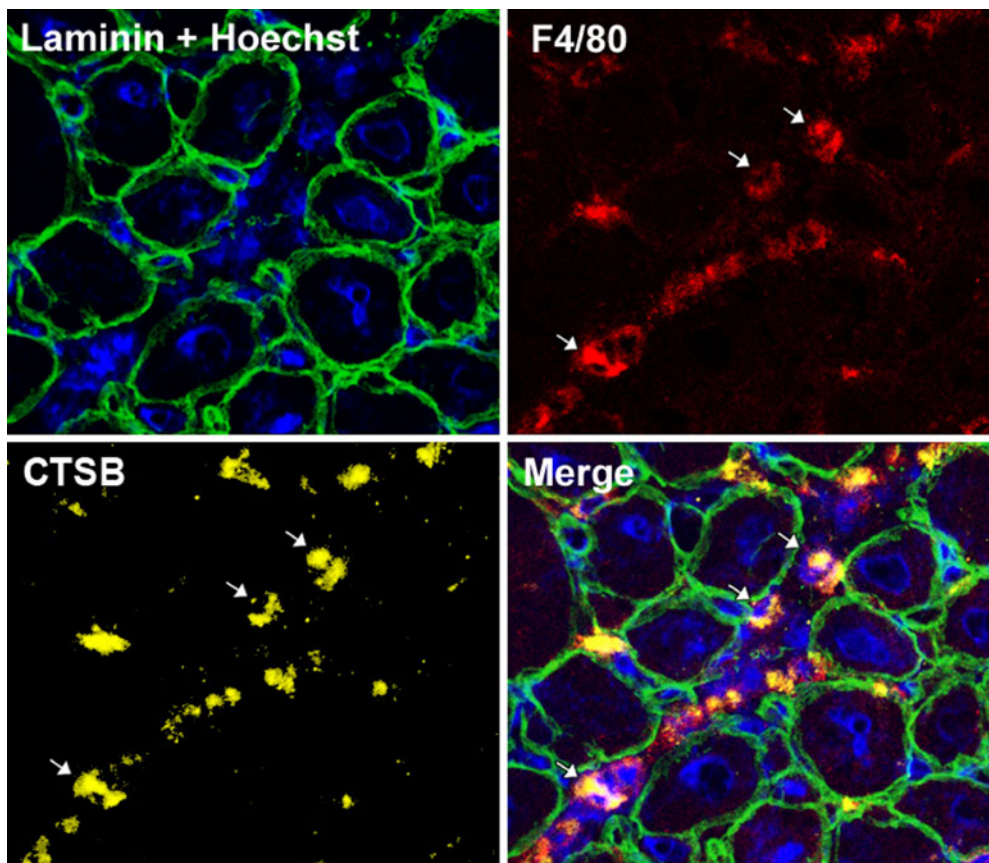

Fig. 3. Inactive CTSB precursor protein localizes to macrophage cytosol. Gastrocnemious muscles taken 5 days post-notexin injection demonstrated the presence of inactive CTSB within the cytosol of macrophages (*white arrows*).
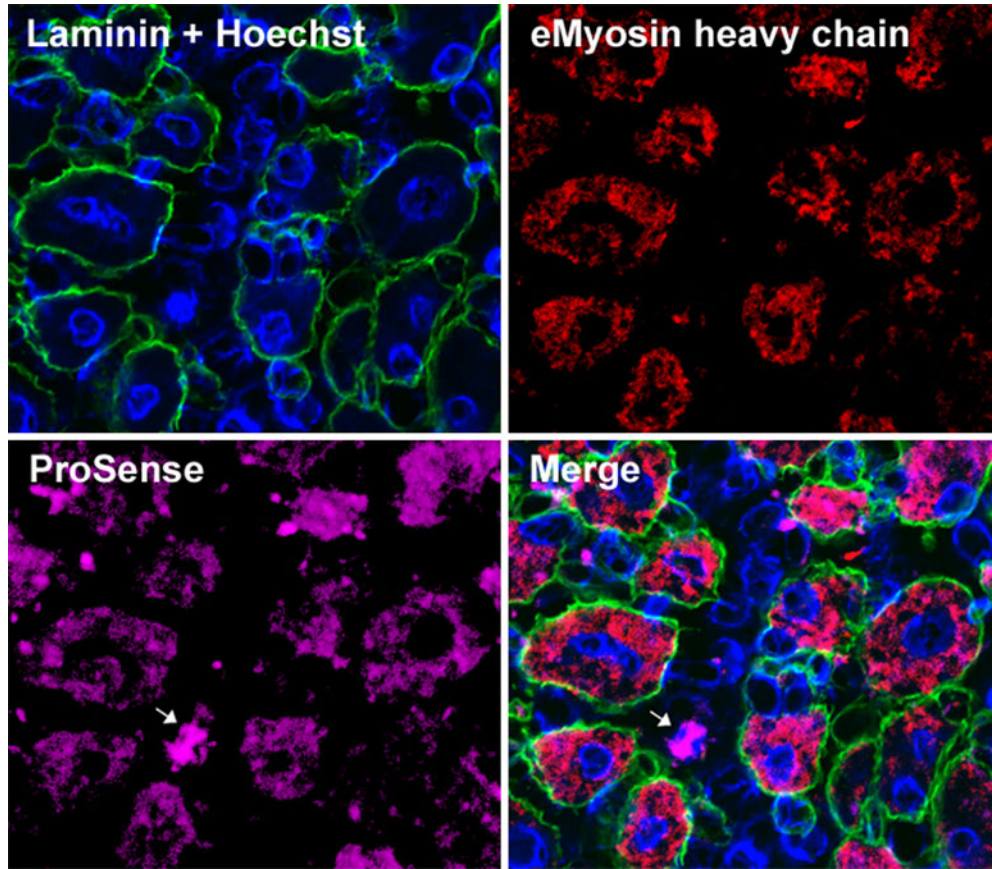
Fig. 4. Activated CTSB primarily localizes within regenerating fibers and macrophages. Gastrocnemious muscles taken 5 days post-notexin injection revealed co-localization of ProSense, which detects activated CTSB, within newly regenerating fibers (eMyosin), as well as within the cytosol of infiltrating monocytes (*white arrow*).
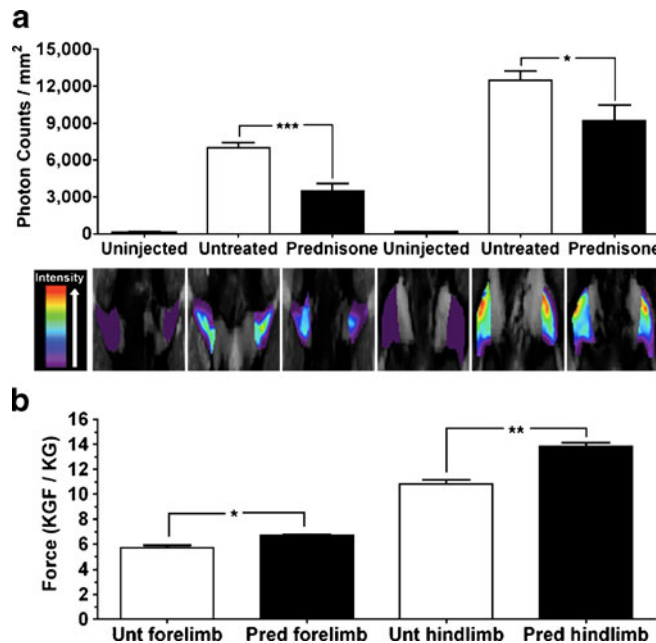

Fig. 5. Prednisone decreases CTSB activity, and correlates with functional improvement. **a**) Prednisone was released continuously in *mdx* mice by placement of a subcutaneous pellet (1 mg/kg) for a total of 3 weeks, and then imaged at baseline without ProSense injection and 24 h after injection. **b**) Grip strength of untreated and mice receiving continuous prednisone was measured after 3 weeks of treatment in the forelimbs and hindlimbs. Student's *t* test, showing standard error of the mean, ***p value of forelimbs=0.0006, *p value of hindlimbs=0.0497.

Table 1. Sample size calculations comparing forelimb and hindlimb between *mdx* and bl10 mice

Measurement	*mdx*	bl10	*N* needed per group to detect a significant difference between mice strains
	Mean total photon counts/mm^2±SD	Mean total photon counts/mm^2±SD	
Forelimb	8,048.33±977.08	2,645.67±1,129.37	1
Hindlimb	14,866.67±2,920.73	8,354.17±2,360.29	3

wanted to encompass the widest range of the disease processes possible, we selected CTSB as our enzymatic marker since it reports on multiple key pathological events relevant to muscle injury. CTSB is secreted by macrophages and activated myoblasts to support the clearance of degenerating injured fibers, as well as promote regeneration via signaling for myoblast fusion [14, 19, 20]. It has already been demonstrated that CTSB protein levels are upregulated in DMD patients as well as in mouse xenograft models, and we further validate this by showing that four encompassing probe sets of the CTSB transcript population are also strongly upregulated (see Supplementary Fig. 1 online) [11, 12]. From the three DMD biopsies that demonstrated the lowest relative levels of CTSB (DMD 3, DMD 4, DMD 11), all had mild histological features such as larger fiber sizes, and minimal amounts of degenerating and regenerating fibers.

ProSense 680 is a commercial near-infrared probe from VisEn Medical and is highly specific for activated CTSB activity. It is normally optically quiescent, but upon reaching areas of activated CTSB, it becomes enzymatically cleaved and emits an intense near-infrared signal. We injected a single 0.75-nmol or 1.5-nmol dose of ProSense 680 I.P. to 5-week-old *mdx* and bl10 mice; this age group was selected because *mdx* mice show peak fiber degeneration and regeneration between 4–10 weeks (see Supplementary Fig. 2 online). Sequential whole body 1.5-mm camera resolution infrared imaging revealed that both bl10 and *mdx* mice had active CTSB in the liver and bladder; however, activity was consistently detected at higher levels in *mdx* limbs compared to bl10 at the 1.5-nmol dose. ProSense levels declined over the course of 7 days, eventually reaching near baseline values, indicating clearance of the probe.

Having determined the peak dose and time point to detect differences in CTSB activity between *mdx* and bl10 limb muscle, we performed high-resolution camera (0.5 mm) imaging of only the forelimbs and hindlimbs 24 h later (Fig. 1a). The CTSB levels were increased in *mdx* tissue over bl10, indicating higher levels of inflammation and regeneration. Moreover, the

higher levels of CTSB activity in *mdx* forelimbs over bl10 forelimbs (3.1-fold increase) compared to *mdx* forelimbs over bl10 hindlimbs (1.9-fold increase) suggested more relative pathology in the forelimbs. Interestingly, this finding is supported by functional grip-strength studies, which clearly demonstrate a greater deficit in grip strength between *mdx* and bl10 mice in the forelimbs over the hindlimbs [21]. Taken together, this suggests that CTSB activity could be inversely related to grip strength. Cryosectioning of quadriceps taken from *mdx* mice that had been injected with ProSense revealed CTSB activity localized specifically to areas of myofiber remodeling (inflammation and regeneration) (Fig. 1b).

We have defined a sensitive method for detecting dystrophic pathology; we therefore wanted to extend its applicability for detecting broader types of muscle injury. Myotoxins such as cardiotoxin and notexin are isolated from snake venom and are highly damaging to myofibers. Intramuscular injection of myotoxins has been shown to induce controlled muscle injury, and, therefore, is useful for studying stage-specific processes in muscle damage and regeneration [22, 23]. Cardiotoxin injection into the gastrocnemius of bl10 mice followed by microarray transcriptional profiling and querying for CTSB revealed that mRNA levels of the enzyme were highest between days 2–5, post injury, with a peak at day 3 (Fig. 2a). Mice that received an intramuscular notexin injection into their right gastrocnemius and were imaged showed an extraordinary amount of activated CTSB at day 1 (Fig. 2b); the levels observed here were more than double that of the *mdx* hindlimb activity shown earlier, demonstrating the severity of acute damage. The peak amount of activated CTSB occurred at day 3, which paralleled mRNA production. By day 14, CTSB approached comparable levels to the saline-injected leg, reflecting the completion of successful myoblast fusion and clearance of infiltrating inflammatory cells. The saline-injected contralateral control leg showed a similar progression in CTSB activity over time, with a peak amount of damage also occurring at day 3, but at much lower levels.

Table 2. Sample-size calculations comparing untreated with prednisone

Measurement	Untreated		Prednisone		*N* needed per group to detect a significant treatment difference
	N	Mean total photon counts/mm^2±SD	*N*	Mean total photon counts/mm^2±SD	
Forelimb	3	7,005.0±977.8	3	3,521.4±911.6	2
Hindlimb	3	12,481.7±1,937.7	3	9,240.2±1,722.8	6

Mean and standard deviations were calculated from the forelimb and hindlimb data in Fig. 1a and Fig. 5a and the number of mice needed per group in order to detect significant differences between strains, and for prednisone treatment was calculated

Upon histological investigation of gastrocnemius muscles from Notexin-injured mice, we found co-localization of the CTSB inactive precursor protein exclusively in infiltrating macrophages, as demonstrated by co-localization between CTSB antibody and F4/80 (Fig. 3). Interestingly, upon imaging of ProSense and embryonic Myosin, heavy-chain, active CTSB was also detected in both infiltrating monocytes and regenerating fibers (Fig. 4). These results substantiate our findings in the quadriceps of 5-week-old *mdx* mice, in that active CTSB is highly localized to areas of myofiber damage, and demonstrate its association with muscle repair, inflammatory, and remodeling processes.

The only effective treatment for DMD discovered to date is glucocorticoids, such as prednisone [24]. Granted that glucocorticoids are ridden with numerous long-term treatment side effects, they are known to reduce both inflammation and excessive muscle degeneration in the short term. We tested our caged CTSB optical method to gauge prednisone's therapeutic effects by administering it for a total of 3 weeks to *mdx* mice in a continuous release pellet, and then performed functional grip-strength tests and optical imaging (Fig. 5). Significant decreases of CTSB activity were measured in both the hindlimbs and forelimbs of prednisone-treated mice, and were accompanied by increases in grip strength (Fig. 5). These data clearly indicate that a decrease in CTSB activity is reflected in an increase in grip-strength measurements at the functional level. The assay described is highly sensitive and specific, requiring only a few animals to see differences between affected and wild-type, or between drug-treated and control dystrophic animals (Tables 1 and 2).

Overall, we found that, under the conditions described, ProSense 680 is a highly effective tool for evaluating *in vivo* assessments of muscle damage, and as a measure of efficacy for drugs designed to reduce inflammation and damage in dystrophic muscle in pre-clinical trials. In the clinic, Optical imaging is beginning to be used more frequently since it doesn't depend on radioactive substances or ionizing radiation, yet provides functional data in a cost-effective manner [25, 26]. The detection of probes using optical imaging also exhibits excellent sensitivity (nmol–pmol range). However, in order to obtain clinically useful results, optical systems and their corresponding probes need to be optimized for monitoring deep tissues due to constraints related to light transmittance and scattering. It would be interesting to see if more powerful therapeutic treatments (e.g., exon skipping, adenovirus gene replacement) could be evaluated using this methodology, and further, if this technology could be applied to DMD patients to gather rapid information on disease progression.

Conflict of Interest. The authors declare that they have no conflict of interest.

References

1. Hoffman EP, Brown RH Jr, Kunkel LM (1987) Dystrophin: the protein product of the Duchenne muscular dystrophy locus. Cell 51:919–928
2. Bulfield G, Siller WG, Wight PA, Moore KJ (1984) X chromosome-linked muscular dystrophy (*mdx*) in the mouse. Proc Natl Acad Sci USA 81:1189–1192
3. Watchko JF, O'Day TL, Hoffman EP (2002) Functional characteristics of dystrophic skeletal muscle: insights from animal models. J Appl Physiol 93:407–417
4. Dunn JF, Zaim-Wadghiri Y (1999) Quantitative magnetic resonance imaging of the mdx mouse model of Duchenne muscular dystrophy. Muscle Nerve 22:1367–1371
5. Lovering RM, McMillan AB, Gullapalli RP (2009) Location of myofiber damage in skeletal muscle after lengthening contractions. Muscle Nerve 40:589–594
6. Brockmann MA, Kemmling A, Groden C (2007) Current issues and perspectives in small rodent magnetic resonance imaging using clinical MRI scanners. Methods 43:79–87
7. Kossodo S et al (2009) Dual *in vivo* quantification of integrin-targeted and protease-activated agents in cancer using fluorescence molecular tomography (FMT). Mol Imaging Biol. doi:10.1007/s11307-009-0279-z
8. Petrof BJ (1998) The molecular basis of activity-induced muscle injury in Duchenne muscular dystrophy. Mol Cell Biochem 179:111–123
9. Briguet A, Courdier-Fruh I, Foster M, Meier T, Magyar JP (2004) Histological parameters for the quantitative assessment of muscular dystrophy in the mdx-mouse. Neuromuscul Disord 14:675–682
10. Jordans S et al (2009) Monitoring compartment-specific substrate cleavage by cathepsins B, K, L, and S at physiological pH and redox conditions. BMC Biochem 10:23
11. Kar NC, Pearson CM (1978) Muscular dystrophy and activation of proteinases. Muscle Nerve 1:308–313
12. Takeda A et al (1992) Demonstration of cathepsins B, H and L in xenografts of normal and Duchenne-muscular-dystrophy muscles transplanted into nude mice. Biochem J 288(Pt 2):643–648
13. Mach L, Stuwe K, Hagen A, Ballaun C, Glossl J (1992) Proteolytic processing and glycosylation of cathepsin B. The role of the primary structure of the latent precursor and of the carbohydrate moiety for cell-type-specific molecular forms of the enzyme. Biochem J 282(Pt 2):577–582
14. Jane DT et al (2006) Cathepsin B localizes to plasma membrane caveolae of differentiating myoblasts and is secreted in an active form at physiological pH. Biol Chem 387:223–234
15. Kesari A et al (2008) Dysferlin deficiency shows compensatory induction of Rab27A/Slp2a that may contribute to inflammatory onset. Am J Pathol 173:1476–1487
16. Hamed S, Sutherland-Smith A, Gorospe J, Kendrick-Jones J, Hoffman E (2005) DNA sequence analysis for structure/function and mutation studies in Becker muscular dystrophy. Clin Genet 68:69–79
17. Nahrendorf M et al (2007) Dual channel optical tomographic imaging of leukocyte recruitment and protease activity in the healing myocardial infarct. Circ Res 100:1218–1225
18. Zhao P et al (2002) Slug is a novel downstream target of MyoD. Temporal profiling in muscle regeneration. J Biol Chem 277:30091–30101

19. Gogos JA et al (1996) Gene trapping in differentiating cell lines: regulation of the lysosomal protease cathepsin B in skeletal myoblast growth and fusion. J Cell Biol 134:837–847

20. Duguez S, Bihan MC, Gouttefangeas D, Feasson L, Freyssenet D (2003) Myogenic and nonmyogenic cells differentially express proteinases, Hsc/Hsp70, and BAG-1 during skeletal muscle regeneration. Am J Physiol Endocrinol Metab 285:E206–E215

21. Spurney CF et al (2009) Preclinical drug trials in the mdx mouse: assessment of reliable and sensitive outcome measures. Muscle Nerve 39:591–602

22. Couteaux R, Mira JC, d'Albis A (1988) Regeneration of muscles after cardiotoxin injury. I. Cytological aspects. Biol Cell 62:171–182

23. Gutierrez JM, Cerdas L (1984) Mechanism of action of myotoxins isolated from snake venoms. Rev Biol Trop 32:213–222

24. Manzur AY, Kuntzer T, Pike M, Swan A (2008) Glucocorticoid corticosteroids for Duchenne muscular dystrophy. Cochrane Database Syst Rev CD003725

25. van de Ven S, Wiethoff A, Nielsen T et al (2009) A novel fluorescent imaging agent for diffuse optical tomography of the breast: first clinical experience in patients. Mol Imaging Biol 12:343–348

26. Shiroishi K et al (2010) Decreased muscle oxygenation and increased arterial blood flow in the non-exercising limb during leg exercise. Adv Exp Med Biol 662:379–384